BJR doi: 10.1259/bjr.20130677

Received: 19 October 2013 | Revised: 15 January 2014 | Accepted: 28 January 2014

Cite this article as:
Becker M, Zaidi H. Imaging in head and neck squamous cell carcinoma: the potential role of PET/MRI. Br J Radiol 2014;87:20130677.

REVIEW ARTICLE

Imaging in head and neck squamous cell carcinoma: the potential role of PET/MRI

[1]MINERVA BECKER, MD and [2]HABIB ZAIDI, PhD

[1]Department of Imaging, Division of Radiology, Geneva University Hospital, Geneva, Switzerland
[2]Department of Imaging, Division of Nuclear Medicine, Geneva University Hospital, Geneva, Switzerland

Address correspondence to: Professor Minerva Becker
E-mail: *Minerva.Becker@hcuge.ch*

ABSTRACT

In head and neck oncology, the information provided by positron emission tomography (PET)/CT and MRI is often complementary because both the methods are based on different biophysical foundations. Therefore, combining diagnostic information from both modalities can provide additional diagnostic gain. Debates about integrated PET/MRI systems have become fashionable during the past few years, since the introduction and wide adoption of software-based multimodality image registration and fusion and the hardware implementation of integrated hybrid PET/MRI systems in pre-clinical and clinical settings. However, combining PET with MRI has proven to be technically and clinically more challenging than initially expected and, as such, research into the potential clinical role of PET/MRI in comparison with PET/CT, diffusion-weighted MRI (DW MRI) or the combination thereof is still ongoing. This review focuses on the clinical applications of PET/MRI in head and neck squamous cell carcinoma (HNSCC). We first discuss current evidence about the use of combined PET/CT and DW MRI, and, then, we explain the rationale and principles of PET/MR image fusion before summarizing the state-of-the-art knowledge regarding the diagnostic performance of PET/MRI in HNSCC. Feasibility and quantification issues, diagnostic pitfalls and challenges in clinical settings as well as ongoing research and potential future applications are also discussed.

Pre-therapeutic work-up of head and neck squamous cell carcinoma (HNSCC) requires clinical evaluation, panendoscopy with biopsy and cross-sectional imaging.[1–3] Cross-sectional imaging is indicated to provide accurate staging at the time of diagnosis. This may be achieved using a variety of imaging modalities, including contrast-enhanced CT (CECT), MRI with or without diffusion-weighted (DW) sequences (DW MRI), ultrasonography with or without fine-needle aspiration cytology (FNAC), positron emission tomography (PET)/CT or a combination of these techniques.

During recent years, the technology for both PET/CT and MRI has evolved steadily, resulting in increased image quality, robustness and rapidity of acquisition. By providing combined metabolic and morphological information, PET/CT has significantly improved diagnostic and prognostic information in HNSCC, thereby facilitating patient management.[1,2] Clinical MRI has evolved towards higher field strengths (3 T), faster sequences, whole-body imaging, as well as functional imaging capabilities, including DW MRI and perfusion imaging.[4–10] Despite all these technical advances, considerable expertise is required for the diagnostic interpretation of head and neck imaging studies because of the complex regional anatomy, the variable appearance of primary and recurrent tumours and functional phenomena mimicking disease.

Since information provided by PET/CT and MRI is complementary in many clinical situations, it seems to make sense to combine the two modalities. From a technical point of view, the integration of PET with MRI in one imaging system has proven to be quite complex. However, the first software algorithms for multimodality data fusion and a first generation of hybrid PET/MRI systems are now available for clinical use. Consequently, the discussion about integrated PET/MRI systems has become fashionable, and an initial euphoria has been generated about potential applications of this new hybrid technology in oncological imaging and especially in the head and neck.[11,12] To date, however, facts and scientific data assessing the clinical usefulness of hybrid PET/MRI systems remain scarce, and it appears difficult to assess where PET/MRI may be preferable over PET/CT, DW MRI or the combination of these two powerful modalities. The purpose of the present article is to summarize current evidence about the combined use of PET/CT and MRI in HNSCC, to explain the rationale and principles of PET/MRI data fusion and to review the existing knowledge

regarding the performance of hybrid PET/MRI in clinical head and neck oncology.

CURRENT EVIDENCE ABOUT POSITRON EMISSION TOMOGRAPHY/CT IN HNSCC

PET/CT has established itself as a robust, rapid and reliable technique providing reproducible data even in patients with limited cooperation. Acquisition of a total body CT scan takes only a few seconds and allows unparallelled detection of pulmonary nodules as well as a complete overview of all anatomic regions. The combination of PET and CT is highly synergistic, resulting in increased sensitivity and specificity for tumour staging as well as effective patient management in clinical routine.[13,14] The metabolic information from PET radiotracers can be complemented by the full diagnostic capability of CECT during the same session, although this may not be done in a majority of institutions.[15]

Positron emission tomography radiotracers and quantification issues

PET radiotracers that can be used for PET/CT examinations in HNSCC patients include 18-fludeoxyglucose (FDG) for the quantification of glucose metabolism, 18-fluorothymidine (FLT) for the quantification of tumour cell proliferation, 18-fluoroethyltyrosine (FET) for the quantification of tumour growth-related protein synthesis, as well as new tracers specifically designed for imaging of apoptosis and epidermal growth factor receptor (EGFR).[2] The most commonly used PET radiotracer for HNSCC in clinical routine is FDG. It is a glucose analogue that is taken up by metabolically active tumour cells using facilitated glucose transport. Because FDG is not a specific tracer for HNSCC, it may also become trapped in other cells with high glucose metabolism, including inflammatory lymph nodes, scar tissue or certain benign salivary gland tumours, such as Whartin tumours.

Quantification of tracer uptake is commonly performed in the clinical setting using the standardized uptake value (SUV). The SUV is a semi-quantitative metric defined as the ratio between the tissue radioactivity concentration (in megabecquerel per kilogram) at a time t and the injected radioactivity (in megabecquerel) extrapolated to the same t normalized to body weight (in kilograms) multiplied by a decay correction factor.[16] As reported by several investigators, SUV_{mean} and SUV_{max} metrics are imperfect quantification tools since they depend on a variety of factors, including data acquisition and reconstruction protocols, selection of regions of interest (ROIs) for measurements, statistical noise, partial volume effect and tumour size.[17–19] Therefore, while the SUV derived from static whole-body images is simpler and more clinically feasible than more rigorous kinetic analysis, there are a number of approximations implicit in the use of uptake ratios that may lead to variability and bias. Despite these drawbacks, quantification of tracer uptake by means of SUV is widely used in clinical routine.

Positron emission tomography/CT for staging and restaging of HNSCC

FDG PET/CT and SUV measurements have proven to be highly accurate for the follow-up of HNSCC after radio-chemotherapy,[20,21] allowing reliable exclusion of residual or recurrent disease.[22–24] Although the high sensitivity and high negative predictive value in the treated neck are consistent findings in most reported studies, the specificity and positive predictive value of FDG PET/CT can vary substantially, leading to a considerable number of false-positive assessments.[25]

In the T staging of primary HNSCC, most authors have reported FDG PET/CT to be as sensitive as CT/MRI.[6,14] Some authors, however, have found PET/CT to be slightly superior to CT/MRI,[26,27] the reported sensitivity for oral cavity HNSCC being 96% for PET/CT, 85% for MRI and 78% for CT.[27] Because CECT and MRI have a superior anatomic resolution, current practice is not in favour of routinely using PET/CT for the T staging of primary HNSCC.[14]

Regarding the staging of nodal disease in primary HNSCC, FDG PET/CT appears to be superior to conventional anatomic MRI sequences.[28,29] However, direct comparison with DW MRI is still missing. Occult lymph nodes in the clinically negative neck (clinical N0 disease) represent a diagnostic challenge for PET/CT and MRI, as both techniques are not sensitive enough to reliably detect subcentimetre metastatic nodes.[15,26,30,31] In skilled hands, ultrasonography has been shown to be superior to CT and MRI because of its high spatial resolution and the ability to routinely perform power Doppler and ultrasonography FNAC.[3] The superiority of ultrasonography FNAC over CT and MRI is indisputable when dealing with small metastatic neck nodes,[32] and ultrasonography FNAC performs significantly better than any other imaging technique in the N0 neck.[3,32] Nevertheless, it is important to realize that micrometastases, which may occur in up to 8% of all N0 necks, are beyond detection by any currently available imaging modality.[3] Several authors have shown that FDG uptake will increase significantly over time in lymph nodes harbouring metastatic cancer lesions, whereas inflammatory neck nodes tend to show a decreased or stable FDG activity over time.[33,34] However, as recently shown, the use of dynamic PET/CT examinations performed between 60 and 115 min after injection of FDG does not allow correct identification of those patients in whom elective neck dissection should be performed.[35] Therefore, most authors currently agree that FDG PET/CT, CECT, MRI or ultrasonography FNAC are not reliable enough to exclude lymph node metastases in the clinical N0 neck.[35,36]

There is general agreement that FDG PET/CT is the method of choice to detect distant metastases and synchronous tumours.[30,37] In locally advanced disease and in patients with N2 or N3 necks, PET/CT may reveal distant metastases and second primary tumours in up to 14% of cases.[38] However, false-positive assessments have also been reported in up to 25% of patients.[14]

The utility of PET/CT to identify unknown primary tumours in patients with metastatic neck nodes has been demonstrated by several reports,[14,39] and PET/CT may be currently recommended early in the work-up of these patients.[14]

Positron emission tomography/CT for radiotherapy planning

Last but not least, with the emergence of new high-precision radiotherapy techniques, such as intensity-modulated radiation

therapy (IMRT), three-dimensional conformal radiotherapy (3D-CRT) or proton beam therapy, PET/CT may play an important role in radiation therapy planning, although contouring the outline of the tumour or metastatic lymph nodes applying PET/CT, the so-called "dose painting", is still one of the most challenging and controversial issues in radiation therapy planning.[14,30,40] Because changing the PET window level can lead to over- or underestimation of the target volume, several groups have suggested different methods for tumour volume contouring, such as normalized volumes according to liver uptake, arbitrary SUV thresholds, 50% of tumour SUV_{max} values, institutional contouring protocols and gradient-based methods.[14]

CURRENT EVIDENCE ABOUT MRI IN HNSCC

Despite the advantages and popularity of PET/CT, there are some shortcomings in the use of CT as the complementary anatomical imaging modality. First of all, CT adds radiation dose to the general examination,[41] particularly when used in a full diagnostic mode. Second, CT provides relatively poor soft-tissue contrasts especially when using low-dose PET/CT acquisition protocols or when intravenous contrast material is not administered.

Utility of morphological MRI sequences in HNSCC

MRI has been shown to be superior to CT for obtaining excellent soft-tissue contrast and for providing images of good quality even in the presence of dental hardware. Conventional MRI sequences are also superior to CT for a variety of findings that influence the therapeutic choice such as laryngeal cartilage invasion, invasion of the skull base, perineural spread, detection of retropharyngeal lymph nodes in nasopharyngeal carcinoma, extranodal spread in metastatic neck nodes and vascular and lymphatic invasion.[4,5,42–44] The introduction of more refined MRI criteria based on the analysis of signal intensity and enhancement patterns after injection of gadolinium chelates has had a major impact on the assessment of deep tumour spread. In most HNSCCs, the actual invasion of bony and cartilaginous structures is often preceded by tumour-induced inflammation.[45] In laryngeal and hypopharyngeal HNSCCs, careful analysis of signal intensities on T_1 and T_2 sequences has improved differentiation between tumour and inflammation: moderate enhancement after injection of gadolinium chelates and moderately high signal on T_2 indicate tumour involvement, whereas high signal on T_2 and strong enhancement correspond histologically to peritumoral inflammation.[4] These diagnostic criteria thereby improve the specificity of MRI for the detection of laryngeal cartilage invasion without affecting its high sensitivity. In analogy, the same criteria can be applied to the skull base or mandible.[46] As suggested by some investigators, differentiation of tumour from peritumoral inflammation can also affect prognosis after radiation therapy.[5,47,48] A moderately high signal within cartilage correlates with a less favourable response to radiation therapy in glottic squamous cell carcinoma (SCC), whereas a high signal on T_2 does not affect local control.[47] It therefore appears that the differentiation of peritumoral inflammation from tumour on the basis of MRI signal intensity characteristics may have direct implications for patient outcome after radiation therapy.[46,47]

Morphological MRI also appears to provide a higher accuracy than FDG PET/CT in detecting residual and/or recurrent nasopharyngeal carcinoma at the primary site and, in the context of tumour restaging, the combination of PET/CT and MRI seems to be superior to either modality alone.[49]

Principles of diffusion-weighted MRI

In addition to providing excellent anatomical detail, MRI has the capability to evaluate functional parameters *in vivo*. DW MRI is a functional MRI technique based on the assessment of random (Brownian) motion of water molecules. In the presence of biological barriers, such as fibres, cell membranes and macromolecules, the free displacement (diffusion) of water molecules is impaired (restricted diffusivity). DW MRI enables *in vivo* imaging and quantification of the diffusivity of water molecules. Images obtained with DW MRI provide a high lesion-to-background contrast, thus outperforming conventional T_2 sequences.[50] Cellular swelling in stroke, increased cellularity in tumours, inflammation and abscesses all lead to a restricted diffusivity. However, restricted diffusivity can also be seen in normal structures such as Waldeyer's ring or normal lymph nodes because these structures have high cellularity.[50] On the other hand, apoptosis and tumour necrosis can lead to decreased cellularity resulting in an increased diffusivity.[7] A drawback of DW MRI is the lack of anatomical information at high b values because of suppressed signal in many normal tissues.[7,50] Therefore, DW MRI should not be interpreted alone but in correlation with morphological sequences or by performing fusion of DW MRI and morphologic MR images (see Pitfalls in hybrid positron emission tomography/MRI).

Quantification issues in diffusion-weighted MRI

Diffusion in biological tissue is quantified by the apparent diffusion coefficient (ADC), which is independent of the strength of the magnetic field.[51–54] Having measured at least two different b values, the logarithm of the relative signal intensity of a tissue is plotted on the y-axis against the b values on the x-axis. The slope of the line fitted through the plots describes the ADC. This mono-exponential fitting represents a rough approximation of ADC and is most often used in clinical routine.[7,54,55] Multiexponential models using several b values are more suitable for quantification; however, the acquisition of multiple b values increases scan duration.[7,55] Mean ADC values (ADC_{mean}) are commonly used for the characterization of HNSCC. Nevertheless, tissue characterization using ADC_{mean} values is not appropriate when the tumour or the metastatic lymph node consist of both highly cellular and poorly cellular or necrotic portions. To overcome this drawback, one should perform ADC_{mean} measurements in areas with high cellularity, or one can use minimum ADC values (ADC_{min}). Further factors that may limit the reliability of ADC measurements include patient motion, image distortion due to magnetic field heterogeneity, artefacts caused by air–soft-tissue interfaces, slice thickness and tissue perfusion. The effect of perfusion is more pronounced with low b values. To overcome the limitations of ADC measurements, the so-called lesion-to-spinal cord ratio (LSR) can be used. It is a semi-quantitative measure calculated by dividing lesion signal intensity by spinal cord signal intensity.[56] LSR has been successfully applied for differentiating benign from malignant lesions in lung cancer patients;[56] however, it is not often used in clinical head and neck imaging. Another approach to evaluate diffusion and perfusion is to calculate and quantify

intravoxel incoherent motion (IVIM)-derived parameters such as D (real diffusion of water molecules), D^* (perfusion contribution to signal decay) or f (perfusion contribution to the diffusion signal).[57–59] IVIM-derived parameters, in particular high initial f values, have been shown to predict a poor prognosis in HNSCC patients[60] and may serve as potential biomarkers in the future. A detailed discussion of IVIM-derived parameters is, however, beyond the scope of this article.

Despite the above-mentioned drawbacks, ADC_{mean} measurements in HNSCC are often used in clinical routine. They have been shown to be reproducible with good to almost perfect inter- and intra-observer agreement.[54,61] Although ADC values cannot predict the histological grade in HNSCC, lower values are observed in poorly differentiated lesions, whereas higher values are seen in well-differentiated tumours.[54,62]

Applications of diffusion-weighted MRI in HNSCC

DW MRI has shown promising results for the nodal staging of primary HNSCC for the assessment of tumour response and prognosis after chemo-radiotherapy and for the detection of recurrent disease.[6–10] Although morphological MRI sequences have a limited performance regarding the detection of nodal metastases,[63] DW MRI with ADC measurements allows detection of subcentimetre metastatic neck nodes.[8] Nevertheless, DW MRI cannot reliably depict nodal metastases <4 mm.[8]

ADC values have also been shown to predict response to treatment: tumours and lymph nodes with lower ADC values are more likely to have a complete response to radio-chemotherapy than lesions with higher ADC values.[64]

Regarding the detection of recurrent disease in the treated neck, DW MRI has shown encouraging results mainly in the larynx and hypopharynx.[10] However, no data are currently available on the value of DW MRI for the staging of recurrent HNSCC (restaging), in particular, as recent reports have suggested that MRI and CT may grossly underestimate the extent of submucosal tumour spread leading to inadequate treatment in many cases.[65,66] Underestimation of submucosal spread in recurrent HNSCC is caused by post-therapeutic inflammation with fibrosis on the one hand and by the fact that recurrent tumours show a different pattern of submucosal spread on the other hand.[65,66] Recurrent tumours typically display a multicentric recurrence pattern with widespread foci of undifferentiated tumour cells as compared with the rather concentric growth pattern of primary carcinomas.[65,66]

PRINCIPLES OF POSITRON EMISSION TOMOGRAPHY/MR IMAGE FUSION AND HYBRID SYSTEMS

When interpreting two different modalities such as MRI and PET from PET/CT, image fusion may be done either visually by the interpreting radiologist or by means of software or hardware fusion. Visual fusion implies that the reader assesses the two modalities side by side on the computer screen and combines the images in his/her mind during interpretation. Interpreting images obtained on two different modalities side by side is time consuming and logistically demanding. Although it has been suggested that side-by-side image interpretation results in diagnostic inaccuracy because of imperfect anatomical matching,[11] there is no scientific evidence currently supporting this view.

The aim of software and hardware fusion is to provide a single integrated image on which a colour-scale functional image (PET) is superimposed on the corresponding anatomical greyscale MR image (typically a contrast-enhanced T_1 or T_2 image). Fusion of PET and MR images requires volume data coregistration from the two modalities. Multimodal image fusion can be generated either by using computerized algorithms enabling coregistration of images obtained on separate systems (PET/CT and MRI) or by hardware coregistration achieved by the use of hybrid PET/MRI devices. Separate systems have the advantage of full temporal and spatial flexibility with independent use of the two devices. However, the challenges and inherent limitations of software-based image registration approaches in whole-body imaging motivated the emergence of hardware-based approaches for multimodality imaging.

Software fusion

Software fusion is technically challenging and can be classified into two categories: rigid and non-rigid. Currently available fusion software typically uses rigid transformation. In this case, the high-resolution anatomical image (reference image) remains stationary, while the low-resolution functional image (source image) is transformed mathematically using geometric parameters (resampled) to match the reference image.[67] Rigid registration may be appropriate for non-moving organs, such as the brain, where the skull provides a rigid structure that preserves the geometrical relationship of structures. However, in the head and neck, rigid registration is not always optimal because of different positioning or breathing. This may result in erroneous interpretation of fused images unless each individual data set is carefully evaluated. To minimize positioning and motion-related misalignment between the two data sets, customized support devices and immobilizing masks may be used during data acquisition whenever very high fusion accuracy, such as for radiotherapy planning, is needed. Non-rigid registration[68] is based on models accounting for the deformable properties of soft tissues (elastic, fluid or other deformation models). These techniques have been used in the clinic with a certain degree of success, but, in most cases, non-rigid image registration can be challenging and, at most institutions, is not used routinely for clinical procedures. In the near future, it is expected that reliable commercial fusion software may enable automatic correction of small differences in data sets caused by breathing or changes in geometrical relationships between different anatomical regions due to positioning differences, in particular in the head and neck area.[69]

Hybrid positron emission tomography/MRI systems

Recently developed hybrid PET/MRI systems allow PET and MRI data sets to be obtained in the same session. The two separate scanners are positioned in-line at a fixed distance, allowing the calibrated data sets to be overlaid with minimal error. Three types of hybrid PET/MRI devices are currently available: simultaneous PET/MRI, sequential PET/MRI and sequential PET/CT-MRI. All

currently available first-generation PET/MRI systems use standard clinical 3-T MRI scanners.

A simultaneous PET/MRI system consists of either a PET insert located between the radiofrequency coil and gradient set of an MRI scanner or a fully integrated and compact design with the two subsystems in the same gantry, thus allowing concomitant PET and MRI data acquisition.[12,70–72] Because photomultiplier tubes used in standard PET scanners do not function properly within or near the strong static magnetic field of MRI scanners, simultaneous PET/MRI scanners use new detector technologies, including avalanche photodiodes (APDs) and silicon photomultiplier tubes (SiPMTs). In addition, electronics are shielded against the static magnetic field, the changing gradients and radiofrequency pulses. Such technology based on APD photodetectors has been implemented on the Biograph mMR hybrid imager (Siemens Healthcare, Erlangen, Germany), the patient being thereby scanned only once.[73,74] Because the coils needed for head and neck imaging can contain amplifier electronics impairing PET image quality, surface coils for simultaneous PET/MRI scanners need to be specifically redesigned. Another challenge in simultaneous PET/MRI is to generate a reliable attenuation map for attenuation correction. Although CT data sets can be easily scaled and used for attenuation correction of PET data since they correlate with electron density, MR image signal intensities are not directly linked to attenuation properties of biological tissues, as they originate from proton spin excitation. Therefore, various approaches have been developed to transform MRI data sets into attenuation maps for PET.[75] These techniques fall into three main categories: segmentation, atlas-based and simultaneous emission/transmission scanning. The first class of techniques is based on segmentation of T_1 weighted or other special MRI sequences.[76–80] Although methods for MRI-based attenuation correction are still a field of intense research, segmentation methods are being utilized clinically,[76–79] while the two other classes of methods are still being explored and developed.

In sequential PET/MRI systems, two separate PET and MRI devices, located within the same room and positioned far enough apart, use a common rotating examination table. The patient is first scanned on one device then the table rotates, and the patient is then scanned on the second device in the same position. Data sets are then fused for clinical interpretation.[81–83] This system has been implemented and is commercially available as the Ingenuity TF PET/MR system (Philips Healthcare, Cleveland, OH). Because of the distance between the two scanners, only minor modifications of PET detectors and MRI surface coils are necessary. Attenuation correction maps are derived from a T_1 MRI sequence.[84,85]

The third option, implemented by GE Healthcare, consists of a tri-modality system composed of a PET/CT and an MRI scanner placed in two adjacent examination rooms with a transferable patient table that can be docked on either of the two systems.[13,86] PET/CT and MRI are performed sequentially, and the patient is shuttled in the same position on the transferable examination table from one room to the other. The acquired PET/CT and MRI are retrospectively coregistered on a commercially available workstation. Images are then displayed as PET/CT, PET/MRI, CT only or PET only.[86] Although this system presents a higher risk for patient motion between the two acquisitions, attenuation correction is done using CT (classical CT-based attenuation correction).

PRE-CLINICAL AND CLINICAL DATA IN THE HEAD AND NECK

Despite the initial excitement related to the implementation of the first PET/MRI scanners in a clinical environment, PET/MRI is still in an early phase of development, and only very few studies have so far addressed the clinical workflow, feasibility and optimized imaging protocols in the head and neck.[12,81,82]

Clinical workflow and protocols

Distant metastases and second primary tumours can occur in a considerable number of patients with advanced primary and recurrent HNSCC.[30,37] Therefore, imaging of HNSCC should not be limited to the head and neck area alone but should additionally cover at least the chest and abdomen. In most institutions, head and neck cancer patients undergoing PET/CT are typically imaged from the head to the pelvic floor. In PET/CT, a low-dose CT is acquired first, followed by a PET acquisition. Depending on institutional protocols, a dedicated total body or regional CECT may be additionally obtained. In analogy to PET/CT, several clinical workflows have been proposed for conducting whole-body PET/MRI studies. One approach is to perform a rapid total body MRI sequence for attenuation correction (typically a T_1 or a Dixon sequence) and to obtain corresponding PET images on bed positions covering the total body. This approach has the advantage of being rapid regardless of the scanner type used (simultaneous or sequential). The total PET/MRI acquisition time in this approach is around 20–40 min. Nevertheless, although sufficient for anatomical localization of focal uptake, this approach is not optimal for the pre-therapeutic evaluation of the head and neck region, as it does not provide the required detailed morphological and functional DW MRI information. In addition, the obtained MR images in the chest are of poorer quality than those obtained with low-dose CT (see below). The second approach consists in performing a rapid total body PET/MRI and an additional full diagnostic high-resolution MRI examination on certain bed positions depending on the clinical situation. This full diagnostic MRI with morphological and DW MRI sequences can be performed, in simultaneous systems, partly during the PET acquisition or, in sequential systems, during the required 60 min necessary for tracer uptake and before the start of the PET acquisition. The simultaneous approach is more time effective than the sequential approach because the morphological MRI can be partially performed during the PET acquisition. Nevertheless, even in the simultaneous approach, not all MRI sequences can be acquired simultaneously with the PET acquisition. Whenever a tripartite PET/CT-MRI system is used, the rapid total body PET/CT is combined with dedicated high-resolution MRI sequences of the clinically relevant regions. Finally, the third approach is to perform a total body full diagnostic high-resolution MRI examination with dedicated sequences in addition to the total body PET acquisition. This option is difficult to implement in clinical routine today because of the unacceptably long acquisition time.

Various PET/MRI protocols for head and neck cancer imaging have been proposed by different investigators, reflecting institutional preferences for sequences and imaging planes, ongoing research protocols, as well as time-effectiveness issues.[77,81,82] Because of cost constraints and limited patient cooperation necessitating a reasonable acquisition time, PET/MRI protocols in head and neck oncology patients will continue to be a compromise between high-resolution imaging including DW MRI and the minimum time lapse necessary for a correct and complete diagnosis. Therefore, it appears desirable to develop standardized PET/MRI protocols that are reproducible across multiple institutions; such attempts are currently made by a few research groups. Last but not least, economic aspects must also be taken into account. Owing to the limited throughput, especially when the full diagnostic MRI potential is used, PET/MRI examinations are likely to be more expensive than PET/CT scans.[13]

Feasibility

Recent studies have shown that PET/MRI is feasible in patients with head and neck tumours on both simultaneous and sequential systems.[12,81,82] In a prospective study, Boss et al[12] assessed the feasibility of FDG PET/MRI in eight patients with head and neck tumours. The patients underwent routine FDG PET/CT followed by PET/MRI performed on a simultaneous hybrid prototype system. No additional FDG and no gadolinium chelates were administered for the PET/MRI examination. The total acquisition time was about 40 min. MRI data sets showed excellent image quality without recognizable artefacts or distortions caused by the inserted PET system.[12] Because of the higher resolution of the PET component of the PET/MRI system in comparison with the PET component of the PET/CT system, PET images from PET/MRI had a superior spatial resolution and improved image contrast compared with images from PET/CT. The authors also performed semi-quantitative analysis, including the calculation of metabolic ratios for normal anatomical structures and for tumours. The metabolic ratios were defined as the ratio of the uptake within the ROI and the mean cerebellar uptake. Boss et al found an excellent agreement between metabolic ratios from both PET systems with correlation coefficients of 0.99 and 0.96 for normal anatomic head and neck structures and tumours, respectively.[12] As the prototype used in this study had a small craniocaudal field of view (only 19 cm), only tumours located at the skull base or in the suprahyoid neck could be imaged. The evaluation of lymph nodes below Level II, of laryngeal or hypopharyngeal cancers as well as of distant metastases and second primary tumours was, however, not possible.[12]

In a review article,[81] we have reported the feasibility of PET/MRI in 221 patients who underwent sequential whole-body FDG PET/MRI with full diagnostic MRI protocols for a variety of indications. The MRI protocols included administration of gadolinium chelates and DW MRI sequences. In 27 head and neck oncology patients, PET/MRI was performed for staging or restaging purposes or for follow-up after radio-chemotherapy.[81] In 3 (11%) cases, PET/MR images could not be interpreted because of motion artefacts and poor image fusion.[81] Moderate fusion quality was present in 4 (15%) cases, hampering the assessment of normal-sized metastatic lymph nodes or HNSCC <2 cm.[81] In the remaining 20 cases (75%), image quality was good with excellent lesion conspicuity. Nevertheless, the reported total examination time was very long (3 h for the dedicated head and neck and total body PET/MRI protocol).

Platzek et al[87] evaluated the feasibility of PET/MRI in the initial staging of 20 head and neck cancer patients and compared the PET images from a sequential PET/MRI system with those obtained on a stand-alone PET scanner. PET/MRI was performed after scanning on the conventional PET system using a single FDG dose. PET/MRI of the head and neck region was feasible on a whole-body PET/MRI system without impairment of PET or MR image quality.[87]

In a prospective study performed in our institution, Varoquaux et al[82] evaluated the feasibility of sequential PET/MRI in 32 head and neck oncology patients. All patients underwent whole-body FDG PET/MRI with a dedicated head and neck examination followed by whole-body PET/CT. The total PET/MRI acquisition time was 90 min. Two experienced observers, who were blinded to clinical data, evaluated the anonymized PET/CT and PET/MRI data sets. Image and fusion quality, lesion conspicuity, anatomical localization of lesions, as well as the number and size of benign and malignant focal uptake lesions were assessed. The quantitative analysis included ROI measurements on both modalities for SUVs of lesions (in the head and neck and rest of the body) and organs. PET/MRI coregistration and image fusion was feasible in all patients initially included in the study.[82] PET/MRI showed equivalent performance to PET/CT regarding rating scores for image quality, fusion quality, lesion conspicuity and anatomical localization, number of detected lesions and number of patients with and without malignant lesions.[82] A high correlation was obtained for SUV values measured on PET/MRI and PET/CT for malignant lesions, benign lesions and organs ($\rho = 0.787$–0.877, $p < 0.001$).

Quantification in hybrid positron emission tomography/MRI

Despite much worthwhile research effort, quantification is still a hot research topic because simultaneous and sequential PET/MRI systems both use MRI-based attenuation correction methods. However, as the tri-modality PET/CT-MRI system employs classical CT-based attenuation correction, the challenges and pitfalls related to MRI-based quantification do not apply. A detailed discussion of ongoing research in the field of MRI-based quantification of tracer uptake is beyond the scope of this article. Nonetheless, performing PET/MRI examinations requires an understanding of the clinically relevant technical issues. Although several groups have demonstrated a statistically significant strong correlation between SUV measurements on PET/MRI and PET/CT,[71,82,88] it was suggested that SUVs of focal uptake and organs might be underestimated on PET/MRI as compared with PET/CT.[71,82,88] Despite differences in study design and data analysis, several investigators have reported that SUV_{mean} for focal uptake may be underestimated by 11–13% on PET/MRI in comparison with its PET/CT counterpart, whereas SUV_{max} appears to be underestimated by 17–20%.[71,82,88] SUVs for normal organs (liver, spleen and bone marrow) also appear to be significantly underestimated by PET/MRI.[71,82,88] As reported by our group, this observed underestimation can result in a limited concordance of

SUV measurements on PET/MRI and PET/CT.[82] Differences in SUVs measured on PET/MRI and PET/CT can be partially attributed to tracer kinetics, as, in all reported studies, PET/MRI and PET/CT were performed sequentially after the administration of a single FDG dose. In the study of Drzezga et al[71] and Wiesmuller et al,[88] PET/CT was performed prior to PET/MRI, whereas in our study PET/MRI was performed first. Therefore, the observed underestimation (similar range in all three studies) cannot be explained by tracer kinetics alone.[82] As MRI-based attenuation correction ignores bone in contrast to CT-based attenuation correction, the observed difference in SUV measurements appears to be particularly pronounced in areas with large bony structures, such as the pelvis and the head and neck.[89] In addition, SUV measurements in malignant tumours appear to be affected by lesion size: the larger the tumour, the bigger the difference in SUVs measured on PET/MRI and PET/CT.[82] Further research is required to better understand differences in SUV measurements on PET/MRI and PET/CT observed in clinical series.

Pitfalls in hybrid positron emission tomography/MRI

Susceptibility artefacts, attenuation correction artefacts and miscoregistration artefacts can hamper the interpretation of head and neck PET/MRI examinations. Susceptibility artefacts occur as the result of microscopic variations in the magnetic field strength near the interfaces of substances with different magnetic susceptibility. Susceptibility artefacts are commonly seen around ferromagnetic objects as contained in dental restorations or osteosynthesis material. Dephasing of spins and frequency shifts in the tissues surrounding the ferromagnetic objects lead to spatial distortion of the surrounding anatomy as well as to bright and dark areas on MRI sequences. These artefacts are more pronounced at high field strength (3 T *vs* 1.5 T), on gradient echo sequences, with long echo train length and DWI sequences. Although metal-based restoration materials can degrade MR image quality, they have an even stronger influence on CT image quality[90] (Figure 1). As suggested by several authors, the observed artefacts are in general larger on CT than on MR images, the size of the artefact mainly depending on the composition of the ferromagnetic material used.[90] A distinct problem is geometric distortion in DW MRI sequences caused by B0 susceptibility differences over the areas imaged. Although parallel imaging techniques reduce geometric distortion, a certain amount of distortion cannot be avoided even with newer DW MRI sequences.[91] Because of miscoregistration of the *k* space, the geometric distortion can be particularly well appreciated when *b* 1000 images are fused with standard morphological sequences.[92] In our experience, this diffeomorphic miscoregistration may result in erroneous interpretation of findings unless morphological MRI sequences are carefully analysed (Figure 2).

Susceptibility artefacts also lead to a void signal on MRI, resulting in wrong assignment of air attenuation coefficient on the corresponding MRI-based attenuation map. It has been suggested to manually "fill the hole" on attenuation correction maps to partially compensate the bias in the estimated SUV values. This most often leads to underestimation of SUV values in PET/MRI.[93] Nevertheless, it is important to point out that artefacts generated by dental implants also have a major impact on SUV values measured on PET/CT.[94,95] In patients with a metal tooth prosthesis, SUVs have been reported to decrease by approximately 20% in the dark streak artefact region and increase by approximately 90% in the bright streak artefact region when compared with the artefact free region.[94] Using a PET/MRI-CT system, Delso et al[96] have reported on the feasibility of correcting dental streak artefacts during CT-based attenuation correction using complementary MRI data.

Motion and respiratory mismatch between the acquisition of MRI and PET data can result in anatomic miscoregistration. Even the slightest degree of miscoregistration can cause diagnostic errors with respect to precise tumour localization (Figure 3) or submucosal extension having a direct impact on tumour staging. Careful analysis of data and comparison with morphological MRI sequences are crucial in order to avoid this interpretation pitfall.

Diagnostic performance of positron emission tomography/MRI in the head and neck

Only very few data are currently available regarding the diagnostic performance in terms of sensitivity, specificity and

Figure 1. This patient was a follow-up case of a squamous cell carcinoma of the floor of the mouth. (a) Axial positron emission tomography (PET)/CT image shows streak artefacts from bilateral dental implants hampering interpretation. Tumour recurrence could not be excluded on the basis of PET/CT. (b) Corresponding hybrid PET/MRI (PET fused with axial gadolinium-enhanced water-only Dixon image) shows the absence of tumour recurrence. In this patient, PET/MRI is less affected by dental artefacts (arrows) than PET/CT.

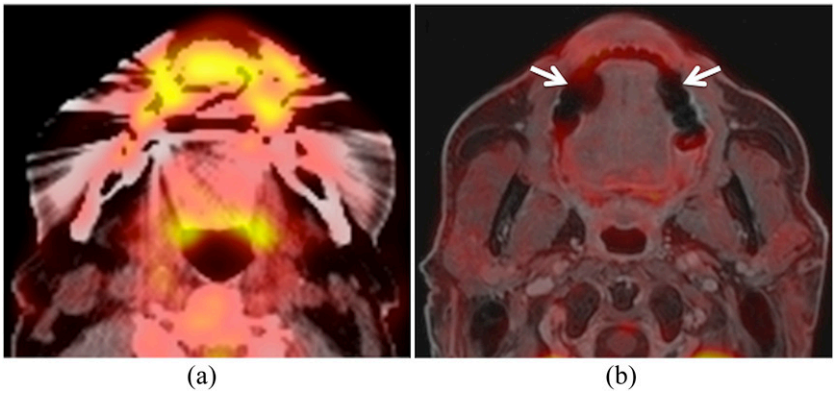

Figure 2. Hybrid positron emission tomography (PET)/MRI obtained for primary staging of advanced laryngeal squamous cell carcinoma. (a) Fused T_2 and *b* 1000 image (colour overlay) illustrate restricted diffusivity in the right Level VI region (arrow), suggesting metastatic lymph nodes. Note geometric distortion of the overlaid *b* 1000 image in comparison with T_2. Position of the spinal cord (long dashed arrow) and T_1 nerve roots (arrowheads) on *b* 1000. Position of the spinal cord on T_2 (short dashed arrow). (b) Corresponding fused T_2 and PET show hypermetabolic thyroid nodule (arrow) and absent Level VI metastatic nodes. Ultrasonography with fine-needle aspiration cytology and surgery revealed a benign thyroid nodule and absent Level VI metastases, respectively.

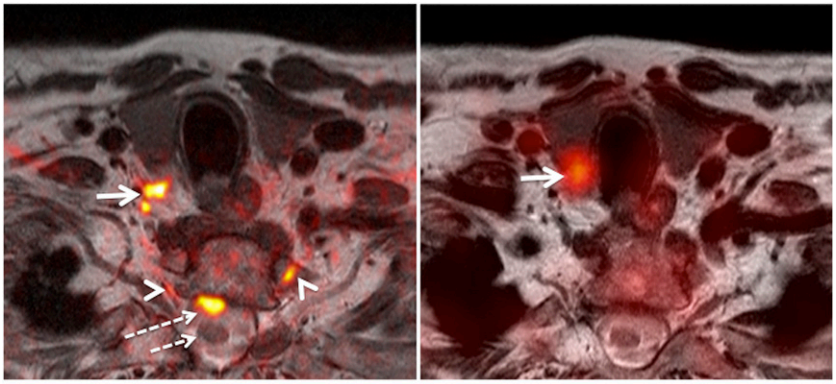

accuracy of PET/MRI in the head and neck.[97–99] These data are based on studies evaluating software fusion of PET and morphological MRI sequences obtained on separate scanners. Nakamoto et al[97] evaluated the clinical value of retrospective image fusion of morphological MRI sequences combined with FDG PET from a stand-alone PET scanner. The study comprised 65 consecutive patients with HNSCC; the standard of reference was histology in 61 patients and follow-up in 4. The sensitivity of MRI and PET/MRI was 98% and 100% for primary tumours, 85% for lymph node metastases and 67% and 92% for recurrent tumours, respectively.[97] The authors concluded that PET/MRI software fusion might be useful in suspected recurrent disease, however no diagnostic gain was obtained in primary tumours.

Huang et al[98] compared the performance of PET/MRI software fusion with PET/CT, MRI and CT for the assessment of deep tissue invasion in 17 patients with advanced buccal SCC. No DW MRI was available. Results were correlated with pathology. The sensitivity and specificity of PET/MRI software fusion were the highest among the four modalities (90%/91% for PET/MRI, 80%/84% for PET/CT, 80%/80% for MRI and 55%/82% for CT, respectively). As the level of diagnostic confidence was also highest for PET/MRI software fusion, Huang et al[98] concluded that, in advanced buccal SCC, PET/MRI is more reliable than PET/CT, MRI or CT for the assessment of local invasion and for the delineation of tumour size.

Kanda et al[99] evaluated the clinical value of retrospective image fusion of MRI and FDG PET from PET/CT in 30 patients with oral cavity and hypopharyngeal SCC. The authors compared the performance of PET/MRI, PET/CT and MRI with histopathology regarding the T and N stage and found that the accuracy for T stage for fused PET/MRI and MRI was similar but superior to PET/CT (87% and 90% *vs* 67%, $p = 0.04$). Regarding N stage, the sensitivity and specificity for the detection of nodal metastasis on a level-per-level basis were 77%/96% for both PET/MRI and PET/CT, compared with 49%/99% for MRI, respectively. The differences in sensitivity ($p = 0.0026$) were significant.[99]

Figure 3. Positron emission tomography (PET)/MRI and PET/CT obtained for primary staging of squamous cell carcinoma of the hypopharynx. (a) Axial PET/CT image shows a hypermetabolic tumour located in the posterior hypopharyngeal wall (arrow). (b) Corresponding hybrid PET/MRI (fused PET and T_2) shows poor data fusion due to patient motion. Note anterior displacement of the PET image in comparison with T_2, suggesting hypermetabolic base of the tongue–vallecula tumour (dashed arrow). True location of the tumour in the hypopharynx (arrow).

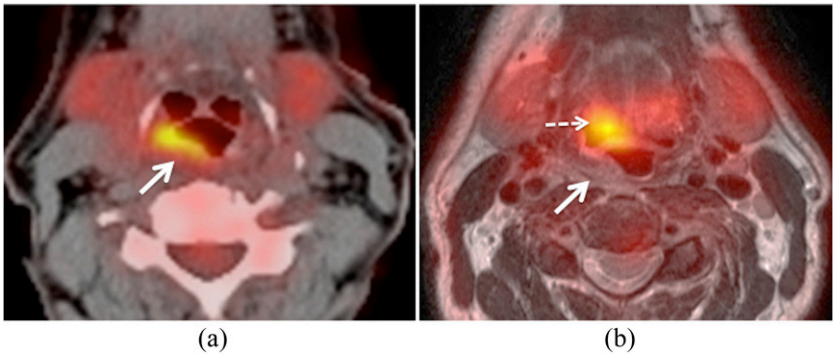

Diagnostic challenges

Despite the above-mentioned encouraging results, interpreting hybrid PET/MRI studies in clinical routine constitutes a diagnostic challenge. Ideally, one would assume that the diagnostic information provided by morphological MRI, DW MRI and PET would be complementary, thereby resulting in a diagnostic gain. Assuming that artefacts have been correctly identified, false-positive and false-negative evaluations with morphological MRI, DW MRI or PET may still occur. How should one deal with discrepant findings between morphological MRI, DW MRI and PET (Figures 4 and 5)? Should one rather "rely on" morphology, DW MRI, perfusion or PET? How can one prospectively identify false-positive and false-negative evaluations with multimodality imaging? False-negative interpretations may have catastrophic consequences for the patient, whereas false positives will result in unnecessary medical procedures and high cost. Only future studies including larger patient series can answer these questions. Although the issue of discrepant PET, MRI and DW MRI findings is not new, hybrid PET/MRI has certainly brought it to the forefront. In our own institution, we are conducting a prospective clinical study to evaluate the performance of PET/MRI in head and neck oncology patients. Based on our preliminary experience, whenever all data are concordant (morphology, DW MRI and PET), the diagnosis is correct (either true positive or true negative) (Figure 6). However, in cases with discordant findings on morphological MRI, DW MRI and PET, we currently recommend endoscopic biopsy, image-guided biopsy or close imaging follow-up depending on the clinical situation. Combined SUV, ADC and perfusion measurements, in particular for lesions interpreted as indeterminate, possibly positive or possibly negative, may facilitate interpretation of findings in the future; multiparametric quantification could ideally be complemented by a decisional algorithm. However, for the time being, no such data exist.

One of the major potential disadvantages of PET/MRI over PET/CT in head and neck cancer patients is due to the fact that MRI is less sensitive than CT for the detection of pulmonary nodules.[100] Appenzeller et al[100] prospectively evaluated whether the performance of PET/MRI using the body coil is sufficient from a diagnostic point of view when compared with standard low-dose non-contrast-enhanced PET/CT regarding the overall diagnostic accuracy, lesion detectability, size and lesion conspicuity. The authors used an axial Dixon-based T_1 weighted 3D gradient echo sequence with a slice thickness of 6.8 mm. Comparison of PET/MRI with PET/CT in 63 patients referred for a variety of malignant tumours revealed a statistically significant superiority of PET/CT over PET/MRI for the conspicuity of pulmonary lesions (p=0.016).[100] The authors suggested that, for this reason, an additional chest CT will probably still remain necessary for most patients in the near future. Nevertheless recent data suggest that PET/MRI may perform somewhat better in this respect.[82] Results from our institution have shown that in head and neck cancer patients PET/MRI may perform as well as PET/CT regarding lung nodule detection provided that a high-resolution Dixon sequence (voxel size 0.85 × 0.85 × 3 mm) is obtained.[82] Nevertheless, the reported data are based on a small number of patients with a low prevalence of lung lesions; further studies in head and neck cancer patients are therefore required to confirm

Figure 4. Hybrid positron emission tomography (PET)/MRI obtained 6 months after radiotherapy of laryngeal squamous cell carcinoma. Clinically, recurrence was suspected. (a) Axial fat-saturated T_2 shows diffuse oedema with posterior commissure involvement (arrow). No evidence of recurrence. (b) Fused T_2 and b 1000 illustrate absent restriction of diffusivity (arrow). Normal high signal of the spinal cord and nerve roots on b 1000. No major geometric distortion. (c) Fused PET and gadolinium-enhanced T_1 show increased 18-fludeoxyglucose uptake (mean standardized uptake value = 3.8; maximum standardized uptake value = 5.2) in the posterior commissure (arrow) suggesting recurrence. Surgical biopsy and follow-up revealed scar tissue.

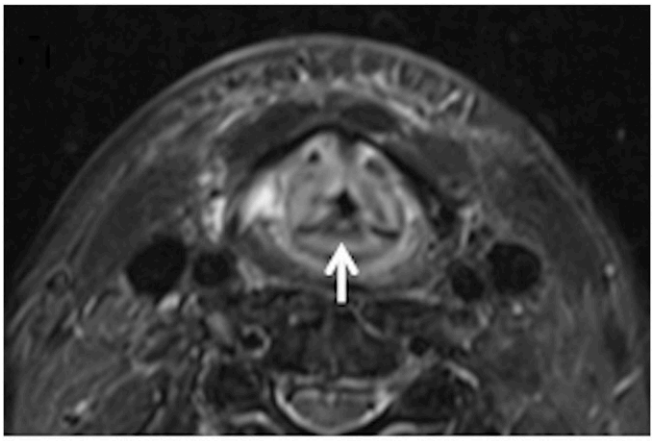

(a)

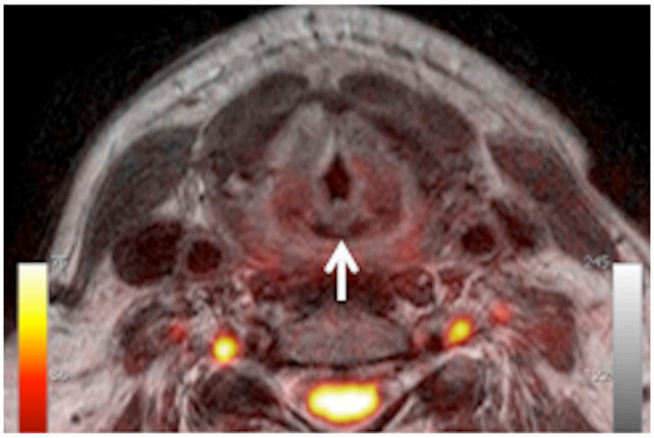

(b)

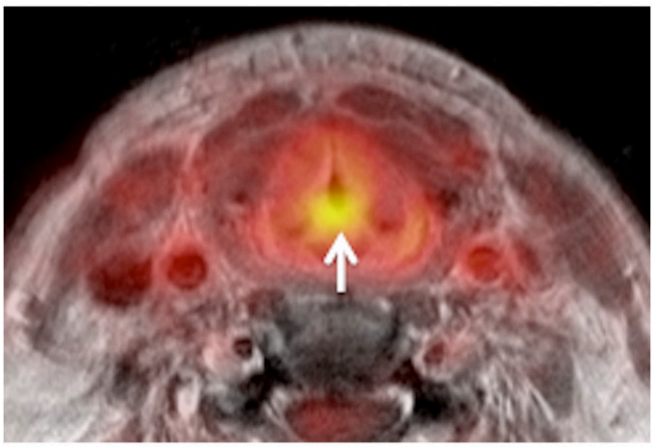

(c)

Figure 5. Hybrid positron emission tomography (PET)/MRI obtained 6 months after proton therapy and chemotherapy for undifferentiated sinonasal carcinoma. Recurrence in the nasopharynx was suspected clinically. (a) Axial fat-saturated gadolinium-enhanced T_1 shows a large nasopharyngeal mass (asterisk) with extensive destruction of the clivus (arrow) and central skull base, suggesting recurrence *vs* radiation-induced inflammation. (b) Apparent diffusion coefficient (ADC) map reveals restricted diffusivity ($ADC_{mean} = 0.98$) suggesting recurrence (asterisks). (c) Corresponding fused PET and gadolinium-enhanced fat-saturated T_1 reveal absent 18-fludeoxyglucose uptake (asterisk) suggesting inflammation. Surgical biopsy and follow-up revealed inflammatory tissue.

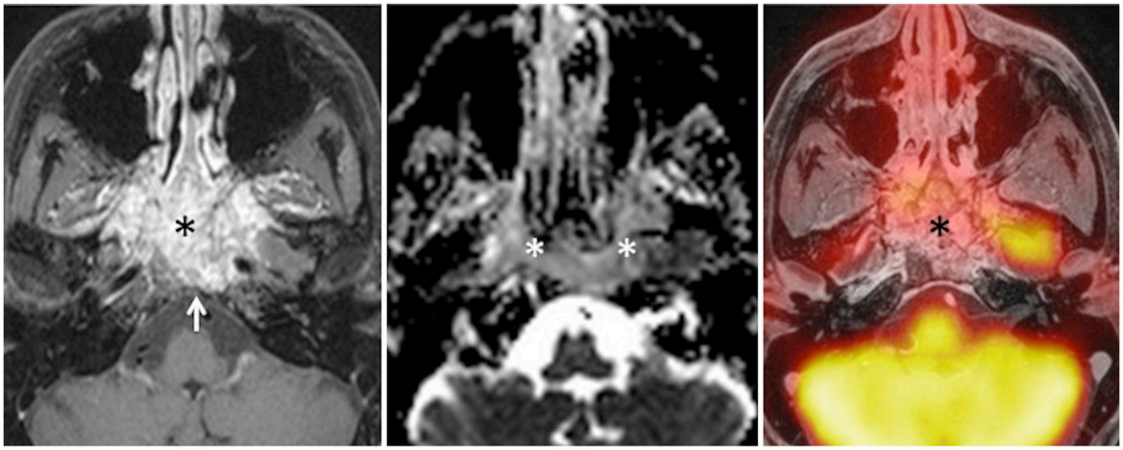

these findings. Our preliminary results in a larger patient series (unpublished data) also show that although the conspicuity of the lung lesions may be less good on PET/MRI than on PET/CT, FDG avid lung nodules are equally well detected with both modalities (Figure 7).

ONGOING RESEARCH AND POTENTIAL FUTURE CLINICAL APPLICATIONS

Ongoing research regarding future clinical applications of PET/MRI in head and neck oncology focuses on the evaluation of the added value of this technique in comparison with the already widely available panoply of diagnostic procedures. In particular, future research involving larger patient series will show whether PET/MRI outperforms PET/CT, MRI, DW MRI or the combination thereof for the detection of metastatic lymph nodes and recurrent disease and for the assessment of treatment response. In addition, combining quantitative parameters from DW MRI, PET and perfusion may add diagnostic certainty and may also prove beneficial for an optimized and individualized treatment plan. A particular challenge for future research consists in developing

Figure 6. Images obtained from the same hybrid positron emission tomography (PET)/MRI examination as shown in Figure 5. (a) Fused *b* 1000 and gadolinium-enhanced water-only Dixon image show restricted diffusivity in the C2 vertebral body (arrow). (b) Fused PET and gadolinium-enhanced water-only Dixon image illustrate increased 18-fludeoxyglucose uptake (mean standardized uptake value = 4.4; maximum standardized uptake value = 6) in the C2 vertebral body (arrow). Similar findings were present in the vertebral bodies of C3–C6 (not shown). The vertebral bodies had been included in the radiation portal. Nevertheless, bone metastases were suspected. (c) Sagittal maximum enhancement perfusion map obtained by dynamic gadolinium-enhanced MRI shows increased vascularization in the vertebral bodies of C2–C6 (in red) supporting the diagnosis of bone metastases. Bone biopsy and follow-up confirmed metastases.

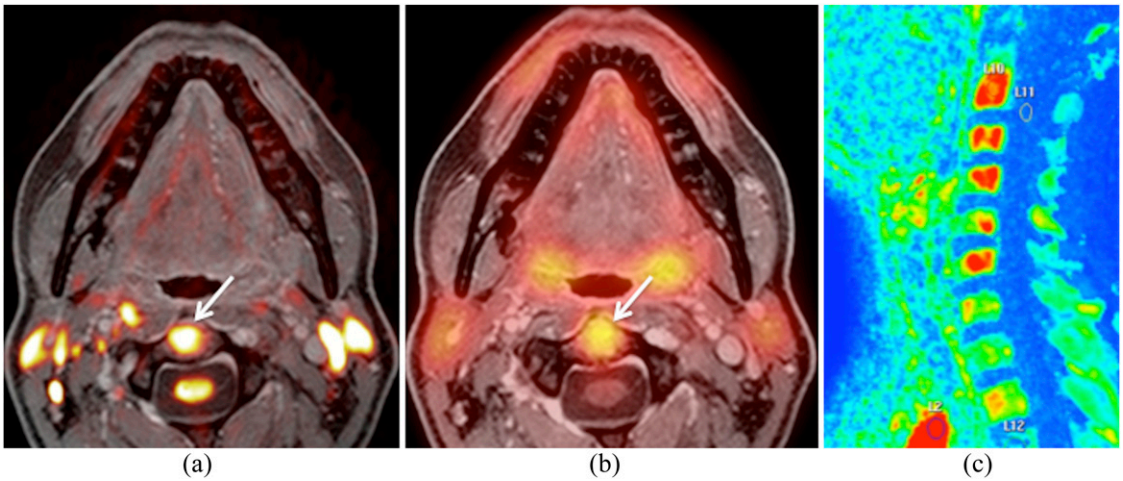

Figure 7. This patient was a follow-up case of a squamous cell carcinoma of the oropharynx. (a) Axial positron emission tomography (PET)/CT shows metastatic mediastinal lymph nodes (dashed arrows) and metastatic lung nodules (arrows). (b) Corresponding hybrid PET/MRI (fused PET and gadolinium-enhanced water-only Dixon image and slice thickness of 2 mm) shows similar findings. Metastatic mediastinal nodes (dashed arrows). Lung metastases (arrows). Note that lung nodule conspicuity is slightly better on PET/CT than on PET/MRI.

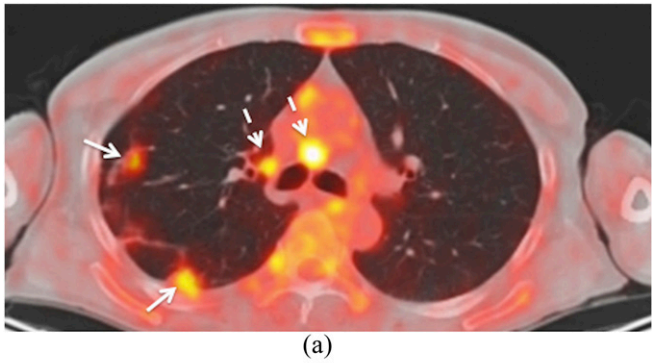

(a)

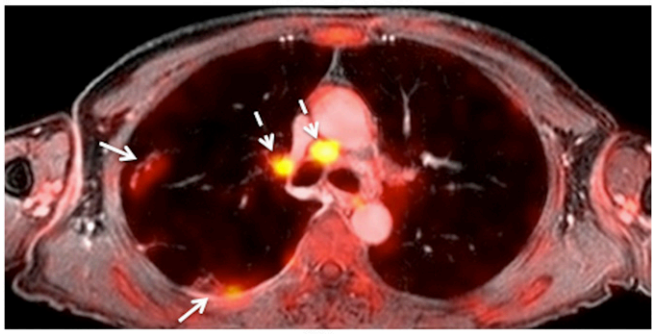

(b)

diagnostic and therapeutic decisional algorithms based on multi-parametric qualitative and quantitative information. The success of ongoing clinical studies will also depend on technical issues, in particular the development of improved quantification algorithms, motion and respiratory compensation software, robust DW MRI sequences with minor geometric distortion, faster high-resolution MRI sequences and, last but not least, economic aspects.

SUMMARY

Although the integration of PET and MRI remains technically complex, this new hybrid imaging modality holds promise because it can combine morphological, functional and molecular information at the same time. We have discussed some of the potential areas where PET/MRI may add diagnostic value to the existing imaging modalities. However, further research is needed to assess the true impact of this technique in HNSCC. Switching clinical workflows to PET/MRI introduces a number of image registration challenges, which were not of major concern with conventional PET/CT scanners. These are linked to the additional artefacts within MRI, the range and number of additional MRI sequences and the range of fields-of-view and orientations of the acquired images. Despite remarkable technical progress in imaging modalities, one must keep in mind that diagnostic interpretation of imaging studies in the context of head and neck tumours remains a challenging task. It demands a great amount of experience and a profound knowledge of the anatomical and functional local changes that may be observed before and after treatment. Because multiple non-invasive imaging studies may sometimes provide contradictory or confusing information, sound clinical judgement is needed to indicate when biopsy may remain the only guide towards correct treatment.

FUNDING

The figures and the preliminary data presented in this review are part of an ongoing clinical study supported by the Swiss National Science Foundation under grants SNF 320030_135728/1 and 31003A_149957.

ACKNOWLEDGMENTS

The authors would like to thank Bénédicte M.A. Delattre, Arthur Varoquaux, Olivier Rager, Osman Ratib, Christoph D. Becker, Pavel Dulguerov, Nicolas Dulguerov, Karim Burkhardt, Angeliki Ailianou, Vincent Lenoir and the entire technical team for their contributions to the Geneva PET/MRI project.

REFERENCES

1. Argiris A, Karamouzis MV, Raben D, Ferris RL. Head and neck cancer. *Lancet* 2008; **371**: 1695–709. doi: 10.1016/S0140-6736(08)60728-X
2. Calabrese L, Ostuni A, Ansarin M, Giugliano G, Maffini F, Alterio D, et al. Future challenges in head and neck cancer: from the bench to the bedside? *Crit Rev Oncol Hematol* 2012; **84**(Suppl. 1): e90–6. doi: 10.1016/j.critrevonc.2010.11.001
3. Richards PS, Peacock TE. The role of ultrasound in the detection of cervical lymph node metastases in clinically N0 squamous cell carcinoma of the head and neck. *Cancer Imaging*. 2007; **7**: 167–78. doi: 10.1102/1470-7330.2007.0024
4. Becker M, Zbären P, Casselman JW, Kohler R, Dulguerov P, Becker CD. Neoplastic invasion of laryngeal cartilage: reassessment of criteria for diagnosis at MR imaging. *Radiology* 2008; **249**: 551–9. doi: 10.1148/radiol.2492072183
5. Becker M, Burkhardt K, Dulguerov P, Allal A. Imaging of the larynx and hypopharynx. *Eur J Radiol* 2008; **66**: 460–79. doi: 10.1016/j.ejrad.2008.03.027
6. Seitz O, Chambron-Pinho N, Middendorp M, Sader R, Mack M, Vogl TJ, et al. 18F-fluorodeoxyglucose-PET/CT to evaluate tumor, nodal disease, and gross tumor volume of oropharyngeal and oral cavity cancer: comparison with MR imaging and validation with surgical specimen. *Neuroradiology* 2009; **51**: 677–86. doi: 10.1007/s00234-009-0586-8
7. Thoeny HC, De Keyzer F, King AD. Diffusion-weighted MR imaging in the head and neck. *Radiology* 2012; **263**: 19–32. doi: 10.1148/radiol.11101821
8. Vandecaveye V, De Keyzer F, Vander Poorten V, Dirix P, Verbeken E, Nuyts S, et al. Head and neck squamous cell carcinoma: value of diffusion-weighted MR imaging for nodal staging.

Radiology 2009; **251**: 134–46. doi: 10.1148/radiol.2511080128

9. Vandecaveye V, Dirix P, De Keyzer F, Op de Beeck K, Vander Poorten V, Hauben E, et al. Diffusion-weighted magnetic resonance imaging early after chemoradiotherapy to monitor treatment response in head-and-neck squamous cell carcinoma. *Int J Radiat Oncol Biol Phys* 2012; **82**: 1098–107. doi: 10.1016/j.ijrobp.2011.02.044
10. Tshering Vogel DW, Zbaeren P, Geretschlaeger A, Vermathen P, De Keyzer F, Thoeny HC. Diffusion-weighted MR imaging including bi-exponential fitting for the detection of recurrent or residual tumour after (chemo)radiotherapy for laryngeal and hypopharyngeal cancers. *Eur Radiol* 2013; **23**: 562–9.
11. Pichler BJ, Kolb A, Nagele T, Schlemmer HP. PET/MRI: paving the way for the next generation of clinical multimodality imaging applications. *J Nucl Med* 2010; **51**: 333–6. doi: 10.2967/jnumed.109.061853
12. Boss A, Stegger L, Bisdas S, Kolb A, Schwenzer N, Pfister M, et al. Feasibility of simultaneous PET/MR imaging in the head and upper neck area. *Eur Radiol* 2011; **21**: 1439–46. doi: 10.1007/s00330-011-2072-z
13. von Schulthess GK, Kuhn FP, Kaufmann P, Veit-Haibach P. Clinical positron emission tomography/magnetic resonance imaging applications. *Semin Nucl Med* 2013; **43**: 3–10. doi: 10.1053/j.semnuclmed.2012.08.005
14. Al-Ibraheem A, Buck A, Krause BJ, Scheidhauer K, Schwaiger M. Clinical applications of FDG PET and PET/CT in head and neck cancer. *J Oncol* 2009; **2009**: 208725. doi: 10.1155/2009/208725
15. Haerle SK, Strobel K, Ahmad N, Soltermann A, Schmid DT, Stoeckli SJ. Contrast-enhanced (1)(8)F-FDG-PET/CT for the assessment of necrotic lymph node metastases. *Head Neck* 2011; **33**: 324–9. doi: 10.1002/hed.21447
16. Huang SC. Anatomy of SUV. Standardized uptake value. *Nucl Med Biol* 2000; **27**: 643–6.
17. Hickeson M, Yun M, Matthies A, Zhuang H, Adam LE, Lacorte L, et al. Use of a corrected standardized uptake value based on the lesion size on CT permits accurate characterization of lung nodules on FDG-PET. *Eur J Nucl Med Mol Imaging* 2002; **29**: 1639–47. doi: 10.1007/s00259-002-0924-0
18. Adams MC, Turkington TG, Wilson JM, Wong TZ. A systematic review of the factors affecting accuracy of SUV measurements. *AJR Am J Roentgenol* 2010; **195**: 310–20. doi: 10.2214/AJR.10.4923
19. Boellaard R, Krak NC, Hoekstra OS, Lammertsma AA. Effects of noise, image resolution, and ROI definition on the accuracy of standard uptake values: a simulation study. *J Nucl Med* 2004; **45**: 1519–27.
20. Brouwer J, Hooft L, Hoekstra OS, Riphagen II, Castelijns JA, de Bree R, et al. Systematic review: accuracy of imaging tests in the diagnosis of recurrent laryngeal carcinoma after radiotherapy. *Head Neck* 2008; **30**: 889–97. doi: 10.1002/hed.20790
21. Isles MG, McConkey C, Mehanna HM. A systematic review and meta-analysis of the role of positron emission tomography in the follow up of head and neck squamous cell carcinoma following radiotherapy or chemoradiotherapy. *Clin Otolaryngol* 2008; **33**: 210–22. doi: 10.1111/j.1749-4486.2008.01688.x
22. Schoder H, Fury M, Lee N, Kraus D. PET monitoring of therapy response in head and neck squamous cell carcinoma. *J Nucl Med* 2009; **50**(Suppl. 1): 74S–88S. doi: 10.2967/jnumed.108.057208
23. Subramaniam RM, Truong M, Peller P, Sakai O, Mercier G. Fluorodeoxyglucose-positron-emission tomography imaging of head and neck squamous cell cancer. *AJNR Am J Neuroradiol* 2010; **31**: 598–604. doi: 10.3174/ajnr.A1760
24. Liu T, Xu W, Yan WL, Ye M, Bai YR, Huang G. FDG-PET, CT, MRI for diagnosis of local residual or recurrent nasopharyngeal carcinoma, which one is the best? A systematic review. *Radiother Oncol* 2007; **85**: 327–35. doi: 10.1016/j.radonc.2007.11.002
25. Yao M, Smith RB, Hoffman HT, Funk GF, Lu M, Menda Y, et al. Clinical significance of postradiotherapy [18F]-fluorodeoxyglucose positron emission tomography imaging in management of head-and-neck cancer: a long-term outcome report. *Int J Radiat Oncol Biol Phys* 2009; **74**: 9–14. doi: 10.1016/j.ijrobp.2008.07.019
26. Ng SH, Yen TC, Chang JT, Chan SC, Ko SF, Wang HM, et al. Prospective study of [18F] fluorodeoxyglucose positron emission tomography and computed tomography and magnetic resonance imaging in oral cavity squamous cell carcinoma with palpably negative neck. *J Clin Oncol* 2006; **24**: 4371–6.
27. Baek CH, Chung MK, Son YI, Choi JY, Kim HJ, Yim YJ, et al. Tumor volume assessment by 18F-FDG PET/CT in patients with oral cavity cancer with dental artifacts on CT or MR images. *J Nucl Med* 2008; **49**: 1422–8. doi: 10.2967/jnumed.108.051649
28. Ng SH, Yen TC, Liao CT, Chang JT, Chan SC, Ko SF, et al. 18F-FDG PET and CT/MRI in oral cavity squamous cell carcinoma: a prospective study of 124 patients with histologic correlation. *J Nucl Med* 2005; **46**: 1136–43.
29. Hustinx R, Lucignani G. PET/CT in head and neck cancer: an update. *Eur J Nucl Med Mol Imaging* 2010; **37**: 645–51. doi: 10.1007/s00259-009-1365-9
30. Iyer NG, Clark JR, Singham S, Zhu J. Role of pretreatment 18FDG-PET/CT in surgical decision-making for head and neck cancers. *Head Neck* 2010; **32**:1202–8. doi: 10.1002/hed.21319
31. Krabbe CA, Balink H, Roodenburg JL, Dol J, de Visscher JG. Performance of 18F-FDG PET/contrast-enhanced CT in the staging of squamous cell carcinoma of the oral cavity and oropharynx. *Int J Oral Maxillofac Surg* 2011; **40**: 1263–70. doi: 10.1016/j.ijom.2011.06.023
32. van den Brekel MW, Castelijns JA, Stel HV, Golding RP, Meyer CJ, Snow GB. Modern imaging techniques and ultrasound-guided aspiration cytology for the assessment of neck node metastases: a prospective comparative study. *Eur Arch Otorhinolaryngol* 1993; **250**: 11–17.
33. Matthies A, Hickeson M, Cuchiara A, Alavi A. Dual time point 18F-FDG PET for the evaluation of pulmonary nodules. *J Nucl Med* 2002; **43**: 871–5.
34. Zhuang H, Pourdehnad M, Lambright ES, Yamamoto AJ, Lanuti M, Li P, et al. Dual time point 18F-FDG PET imaging for differentiating malignant from inflammatory processes. *J Nucl Med* 2001; **42**: 1412–17.
35. Carlson ER, Schaefferkoetter J, Townsend D, McCoy JM, Campbell PD Jr, Long M. The use of multiple time point dynamic positron emission tomography/computed tomography in patients with oral/head and neck cancer does not predictably identify metastatic cervical lymph nodes. *J Oral Maxillofac Surg* 2013; **71**: 162–77.
36. Stoeckli SJ, Haerle SK, Strobel K, Haile SR, Hany TF, Schuknecht B. Initial staging of the neck in head and neck squamous cell carcinoma: a comparison of CT, PET/CT, and ultrasound-guided fine-needle aspiration cytology. *Head Neck* 2012; **34**: 469–76. doi: 10.1002/hed.21764
37. Abgral R, Querellou S, Potard G, Le Roux PY, Le Duc-Pennec A, Marianovski R, et al. Does 18F-FDG PET/CT improve the detection of posttreatment recurrence of head and neck squamous cell carcinoma in patients negative for disease on clinical follow-up? *J Nucl Med* 2009; **50**: 24–9. doi: 10.2967/jnumed.108.055806

38. Ng SH, Chan SC, Yen TC, Chang JT, Liao CT, Ko SF, et al. Staging of untreated nasopharyngeal carcinoma with PET/CT: comparison with conventional imaging work-up. *Eur J Nucl Med Mol Imaging* 2009; **36**: 12–22. doi: 10.1007/s00259-008-0918-7
39. Rusthoven KE, Koshy M, Paulino AC. The role of fluorodeoxyglucose positron emission tomography in cervical lymph node metastases from an unknown primary tumor. *Cancer* 2004; **101**: 2641–9. doi: 10.1002/cncr.20687
40. Schinagl DA, Span PN, van den Hoogen FJ, Merkx MA, Slootweg PJ, Oyen WJ, et al. Pathology-based validation of FDG PET segmentation tools for volume assessment of lymph node metastases from head and neck cancer. *Eur J Nucl Med Mol Imaging* 2013; **40** 1828–35. doi: 10.1007/s00259-013-2513-9
41. Chawla SC, Federman N, Zhang D, Nagata K, Nuthakki S, McNitt-Gray M, et al. Estimated cumulative radiation dose from PET/CT in children with malignancies: a 5-year retrospective review. *Pediatr Radiol* 2010; **40**: 681–6. doi: 10.1007/s00247-009-1434-z
42. Maroldi R, Farina D, Borghesi A, Marconi A, Gatti E. Perineural tumor spread. *Neuroimaging Clin N Am* 2008; **18**: 413–29, xi. doi: 10.1016/j.nic.2008.01.001
43. Ljumanovic R, Langendijk JA, Hoekstra OS, Leemans CR, Castelijns JA. Distant metastases in head and neck carcinoma: identification of prognostic groups with MR imaging. *Eur J Radiol* 2006; **60**: 58–66. doi: 10.1016/j.ejrad.2006.05.019
44. Zhang GY, Liu LZ, Wei WH, Deng YM, Li YZ, Liu XW. Radiologic criteria of retropharyngeal lymph node metastasis in nasopharyngeal carcinoma treated with radiation therapy. *Radiology* 2010; **255**: 605–12.
45. Becker M, Zbaren P, Laeng H, Stoupis C, Porcellini B, Vock P. Neoplastic invasion of the laryngeal cartilage: comparison of MR imaging and CT with histopathologic correlation. *Radiology* 1995; **194**: 661–9. doi: 10.1148/radiology.194.3.7862960
46. Curtin HD. The "evil gray": cancer and cartilage. *Radiology* 2008; **249**: 410–12. doi: 10.1148/radiol.2492081113
47. Ljumanovic R, Langendijk JA, van Wattingen M, Schenk B, Knol DL, Leemans CR, et al. MR imaging predictors of local control of glottic squamous cell carcinoma treated with radiation alone. *Radiology* 2007; **244**: 205–12. doi: 10.1148/radiol.2441060593
48. Ljumanovic R, Langendijk JA, Hoekstra OS, Knol DL, Leemans CR, Castelijns JA. Pre- and post-radiotherapy MRI results as a predictive model for response in laryngeal carcinoma. *Eur Radiol* 2008; **18**: 2231–40. doi: 10.1007/s00330-008-0986-x
49. Comoretto M, Balestreri L, Borsatti E, Cimitan M, Franchin G, Lise M. Detection and restaging of residual and/or recurrent nasopharyngeal carcinoma after chemotherapy and radiation therapy: comparison of MR imaging and FDG PET/CT. *Radiology* 2008; **249**: 203–11. doi: 10.1148/radiol.2491071753
50. Kwee TC, Takahara T, Ochiai R, Koh DM, Ohno Y, Nakanishi K, et al. Complementary roles of whole-body diffusion-weighted MRI and 18F-FDG PET: the state of the art and potential applications. *J Nucl Med* 2010; **51**: 1549–58. doi: 10.2967/jnumed.109.073908
51. Koh DM, Collins DJ. Diffusion-weighted MRI in the body: applications and challenges in oncology. *AJR Am J Roentgenol* 2007; **188**: 1622–35. doi: 10.2214/AJR.06.1403
52. Kim S, Loevner L, Quon H, Sherman E, Weinstein G, Kilger A, et al. Diffusion-weighted magnetic resonance imaging for predicting and detecting early response to chemoradiation therapy of squamous cell carcinomas of the head and neck. *Clin Cancer Res* 2009; **15**: 986–94. doi: 10.1158/1078-0432.CCR-08-1287
53. Fushimi Y, Miki Y, Okada T, Yamamoto A, Mori N, Hanakawa T, et al. Fractional anisotropy and mean diffusivity: comparison between 3.0-T and 1.5-T diffusion tensor imaging with parallel imaging using histogram and region of interest analysis. *NMR Biomed* 2007; **20**: 743–8.
54. Varoquaux A, Rager O, Lovblad KO, Masterson K, Dulguerov P, Ratib O, et al. Functional imaging of head and neck squamous cell carcinoma with diffusion-weighted MRI and FDG PET/CT: quantitative analysis of ADC and SUV. *Eur J Nucl Med Mol Imaging* 2013; **40**: 842–52. doi: 10.1007/s00259-013-2351-9
55. Koh DM, Blackledge M, Padhani AR, Takahara T, Kwee TC, Leach MO, et al. Whole-body diffusion-weighted MRI: tips, tricks, and pitfalls. *AJR Am J Roentgenol* 2012; **199**: 252–62. doi: 10.2214/AJR.11.7866
56. Uto T, Takehara Y, Nakamura Y, Naito T, Hashimoto D, Inui N, et al. Higher sensitivity and specificity for diffusion-weighted imaging of malignant lung lesions without apparent diffusion coefficient quantification. *Radiology* 2009; **252**: 247–54.
57. Le Bihan D, Breton E, Lallemand D, Aubin ML, Vignaud J, Laval-Jeantet M. Separation of diffusion and perfusion in intravoxel incoherent motion MR imaging. *Radiology* 1988; **168**: 497–505. doi: 10.1148/radiology.168.2.3393671
58. Martínez Barbero J, Rodríquez Jiménez I, Martin Noguerol T, Luna Alcalá A. Utility of MRI diffusion techniques in the evaluation of tumors of the head and neck. *Cancers* 2013; **5**: 875–89. doi: 10.3390/cancers5030875
59. Rheinheimer S, Stieltjes B, Schneider F, Simon D, Pahernik S, Kauczor HU, et al. Investigation of renal lesions by diffusion-weighted magnetic resonance imaging applying intravoxel incoherent motion-derived parameters: initial experience. *Eur J Radiol* 2012; **81**: e310–16.
60. Hauser T, Essig M, Jensen A, Gerigk L, Laun FB, Munter M, et al. Characterization and therapy monitoring of head and neck carcinomas using diffusion-imaging-based intravoxel incoherent motion parameters: preliminary results. *Neuroradiology* 2013; **55**: 527–36.
61. Verhappen MH, Pouwels PJ, Ljumanovic R, van der Putten L, Knol DL, De Bree R, et al. Diffusion-weighted MR imaging in head and neck cancer: comparison between half-Fourier acquired single-shot turbo spin-echo and EPI techniques. *AJNR Am J Neuroradiol* 2012; **33**: 1239–46. doi: 10.3174/ajnr.A2949
62. Ichikawa Y, Sumi M, Sasaki M, Sumi T, Nakamura T. Efficacy of diffusion-weighted imaging for the differentiation between lymphomas and carcinomas of the nasopharynx and oropharynx: correlations of apparent diffusion coefficients and histologic features. *AJNR Am J Neuroradiol* 2012; **33**: 761–6.
63. Curtin HD, Ishwaran H, Mancuso AA, Dalley RW, Caudry DJ, McNeil BJ. Comparison of CT and MR imaging in staging of neck metastases. *Radiology* 1998; **207**: 123–30. doi: 10.1148/radiology.207.1.9530307
64. Herneth AM, Mayerhoefer M, Schernthaner R, Ba-Ssalamah A, Czerny Ch, Fruehwald-Pallamar J. Diffusion weighted imaging: lymph nodes. *Eur J Radiol* 2010; **76**: 398–406. doi: 10.1016/j.ejrad.2010.08.016
65. Zbaren P, Nuyens M, Curschmann J, Stauffer E. Histologic characteristics and tumor spread of recurrent glottic carcinoma: analysis on whole-organ sections and comparison with tumor spread of primary glottic carcinomas. *Head Neck* 2007; **29**: 26–32.
66. Zbaren P, Christe A, Caversaccio MD, Stauffer E, Thoeny HC. Pretherapeutic staging of recurrent laryngeal carcinoma: clinical findings and imaging studies

compared with histopathology. *Otolaryngol Head Neck Surg* 2007; **137**: 487–91.
67. Pietrzyk U, Herholz K, Fink G, Jacobs A, Mielke R, Slansky I, et al. An interactive technique for three-dimensional image registration: validation for PET, SPECT, MRI and CT brain studies. *J Nucl Med* 1994; **35**:2011–18.
68. Leibfarth S, Monnich D, Welz S, Siegel C, Schwenzer N, Schmidt H, et al. A strategy for multimodal deformable image registration to integrate PET/MR into radiotherapy treatment planning. *Acta Oncol* 2013; **52**: 1353–9. doi: 10.3109/0284186X.2013.813964
69. Schoenfeld JD, Kovalchuk N, Subramaniam RM, Truong MT. PET/CT of cancer patients: part 2, deformable registration imaging before and after chemotherapy for radiation treatment planning in head and neck cancer. *AJR Am J Roentgenol* 2012; **199**: 968–74.
70. Wurslin C, Schmidt H, Martirosian P, Brendle C, Boss A, Schwenzer NF, et al. Respiratory motion correction in oncologic PET using T1-weighted MR imaging on a simultaneous whole-body PET/MR system. *J Nucl Med* 2013; **54**: 464–71. doi: 10.2967/jnumed.112.105296
71. Drzezga A, Souvatzoglou M, Eiber M, Beer AJ, Fürst S, Martinez-Möller A, et al. First clinical experience with integrated whole-body PET/MR: comparison to PET/CT in patients with oncologic diagnoses. *J Nucl Med* 2012; **53**: 845–55.
72. Buchbender C, Heusner TA, Lauenstein TC, Bockisch A, Antoch G. Oncologic PET/MRI, part 1: tumors of the brain, head and neck, chest, abdomen, and pelvis. *J Nucl Med* 2012; **53**: 928–38. doi: 10.2967/jnumed.112.105338
73. Judenhofer MS, Wehrl HF, Newport DF, Catana C, Siegel SB, Becker M, et al. Simultaneous PET-MRI: a new approach for functional and morphological imaging. *Nat Med* 2008; **14**: 459–65. doi: 10.1038/nm1700
74. Schlemmer HP, Pichler BJ, Schmand M, Burbar Z, Michel C, Ladebeck R, et al. Simultaneous MR/PET imaging of the human brain: feasibility study. *Radiology* 2008; **248**: 1028–35. doi: 10.1148/radiol.2483071927
75. Zaidi H. Is MR-guided attenuation correction a viable option for dual-modality PET/MR imaging? *Radiology* 2007; **244**: 639–42. doi: 10.1148/radiol.2443070092
76. Eiber M, Martinez-Moller A, Souvatzoglou M, Holzapfel K, Pickhard A, Loffelbein D, et al. Value of a Dixon-based MR/PET attenuation correction sequence for the localization and evaluation of PET-positive lesions. *Eur J Nucl Med Mol Imaging* 2011; **38**: 1691–701. doi: 10.1007/s00259-011-1842-9
77. Eiber M, Souvatzoglou M, Pickhard A, Loeffelbein DJ, Knopf A, Holzapfel K, et al. Simulation of a MR-PET protocol for staging of head-and-neck cancer including Dixon MR for attenuation correction. *Eur J Radiol* 2012; **81**: 2658–65. doi: 10.1016/j.ejrad.2011.10.005
78. Delso G, Furst S, Jakoby B, Ladebeck R, Ganter C, Nekolla SG, et al. Performance measurements of the Siemens mMR integrated whole-body PET/MR scanner. *J Nucl Med* 2011; **52**: 1914–22. doi: 10.2967/jnumed.111.092726
79. Martinez-Moller A, Souvatzoglou M, Delso G, Bundschuh RA, Chefd'hotel C, Ziegler SI, et al. Tissue classification as a potential approach for attenuation correction in whole-body PET/MRI: evaluation with PET/CT data. *J Nucl Med* 2009; **50**: 520–6. doi: 10.2967/jnumed.108.054726
80. Wagenknecht G, Kaiser HJ, Mottaghy FM, Herzog H. MRI for attenuation correction in PET: methods and challenges. *MAGMA* 2013; **26**: 99–113. doi: 10.1007/s10334-012-0353-4
81. Vargas MI, Becker M, Garibotto V, Heinzer S, Loubeyre P, Gariani J, et al. Approaches for the optimization of MR protocols in clinical hybrid PET/MRI studies. *MAGMA* 2013; **26**: 57–69. doi: 10.1007/s10334-012-0340-9
82. Varoquaux A, Rager O, Poncet A, Delattre BM, Ratib O, Becker CD, et al. Detection and quantification of focal uptake in head and neck tumours: (18)F-FDG PET/MR versus PET/CT. *Eur J Nucl Med Mol Imaging* 2014; **41**: 462–75. doi: 10.1007/s00259-013-2580-y
83. Ratib O, Beyer T. Whole-body hybrid PET/MRI: ready for clinical use? *Eur J Nucl Med Mol Imaging* 2011; **38**: 992–5. doi: 10.1007/s00259-011-1790-4
84. Zaidi H, Del Guerra A. An outlook on future design of hybrid PET/MRI systems. *Med Phys* 2011; **38**: 5667–89. doi: 10.1118/1.3633909
85. Zaidi H, Ojha N, Morich M, Griesmer J, Hu Z, Maniawski P, et al. Design and performance evaluation of a whole-body Ingenuity TF PET-MRI system. *Phys Med Biol* 2011; **56**: 3091–106. doi: 10.1088/0031-9155/56/10/013
86. Veit-Haibach P, Kuhn FP, Wiesinger F, Delso G, von Schulthess G. PET-MR imaging using a tri-modality PET/CT-MR system with a dedicated shuttle in clinical routine. *MAGMA* 2013; **26**: 25–35. doi: 10.1007/s10334-012-0344-5
87. Platzek I, Beuthien-Baumann B, Schneider M, Gudziol V, Langner J, Schramm G, et al. PET/MRI in head and neck cancer: initial experience. *Eur J Nucl Med Mol Imaging* 2013; **40**: 6–11. doi: 10.1007/s00259-012-2248-z
88. Wiesmuller M, Quick HH, Navalpakkam B, Lell MM, Uder M, Ritt P, et al. Comparison of lesion detection and quantitation of tracer uptake between PET from a simultaneously acquiring whole-body PET/MR hybrid scanner and PET from PET/CT. *Eur J Nucl Med Mol Imaging* 2013; **40**: 12–21. doi: 10.1007/s00259-012-2249-y
89. Bini J, Izquierdo-Garcia D, Mateo J, Machac J, Narula J, Fuster V, et al. Preclinical evaluation of MR attenuation correction versus CT attenuation correction on a sequential whole-body MR/PET scanner. *Invest Radiol* 2013; **48**: 313–22. doi: 10.1097/RLI.0b013e31827a49ba
90. Klinke T, Daboul A, Maron J, Gredes T, Puls R, Jaghsi A, et al. Artifacts in magnetic resonance imaging and computed tomography caused by dental materials. *PLoS One* 2012; **7**: e31766. doi: 10.1371/journal.pone.0031766
91. Huang H, Ceritoglu C, Li X, Qiu A, Miller MI, van Zijl PC, et al. Correction of B0 susceptibility induced distortion in diffusion-weighted images using large-deformation diffeomorphic metric mapping. *Magn Reson Imaging* 2008; **26**: 1294–302. doi: 10.1016/j.mri.2008.03.005
92. Ruthotto L, Kugel H, Olesch J, Fischer B, Modersitzki J, Burger M, et al. Diffeomorphic susceptibility artifact correction of diffusion-weighted magnetic resonance images. *Phys Med Biol* 2012; **57**: 5715–31. doi: 10.1088/0031-9155/57/18/5715
93. Buchbender C, Hartung-Knemeyer V, Forsting M, Antoch G, Heusner TA. Positron emission tomography (PET) attenuation correction artefacts in PET/CT and PET/MRI. *Br J Radiol* 2013; **86**: 20120570. doi: 10.1259/bjr.20120570
94. Park HH, Shin JY, Lee J, Jin GH, Kim HS, Lyu KY, et al. A study on the artifacts generated by dental materials in PET/CT image. *Conf Proc IEEE Eng Med Biol Soc* 2013; **2013**: 2465–8. doi: 10.1109/EMBC.2013.6610039
95. Abdoli M, Ay MR, Ahmadian A, Dierckx RA, Zaidi H. Reduction of dental filling metallic artifacts in CT-based attenuation correction of PET data using weighted virtual sinograms optimized by a genetic algorithm. *Med Phys* 2010; **37**: 6166–77.
96. Delso G, Wollenweber S, Lonn A, Wiesinger F, Veit-Haibach P. MR-driven metal artifact

reduction in PET/CT. *Phys Med Biol* 2013; **58**: 2267–80. doi: 10.1088/0031-9155/58/7/2267

97. Nakamoto Y, Tamai K, Saga T, Higashi T, Hara T, Suga T, et al. Clinical value of image fusion from MR and PET in patients with head and neck cancer. *Mol Imaging Biol* 2009; **11**: 46–53. doi: 10.1007/s11307-008-0168-x
98. Huang S-H, Chien C-Y, Lin W-C, Fang F-M, Wang P-W, Lui C-C, et al. A comparative study of fused FDG PET/MRI, PET/CT, MRI, and CT imaging for assessing surrounding tissue invasion of advanced buccal squamous cell carcinoma. *Clin Nucl Med* 2011; **36**: 518–25. doi: 10.1097/RLU.0b013e318217566f
99. Kanda T, Kitajima K, Suenaga Y, Konishi J, Sasaki R, Morimoto K, et al. Value of retrospective image fusion of F-FDG PET and MRI for preoperative staging of head and neck cancer: comparison with PET/CT and contrast-enhanced neck MRI. *Eur J Radiol* 2013; **82**: 2005–10. doi: 10.1016/j.ejrad.2013.06.025
100. Appenzeller P, Mader C, Huellner MW, Schmidt D, Schmid D, Boss A, et al. PET/CT versus body coil PET/MRI: how low can you go? *Insights Imaging* 2013; **4**: 481–90. doi: 10.1007/s13244-013-0247-7